A Time-Resolved Fluorescence Diphenylhexatriene (DPH) Anisotropy Characterization of a Series of Model Lipid Constructs for the Sperm Plasma Membrane

Gregory M. Troup,[†] Steven P. Wrenn,[‡] Meirav Apel-Paz,[†] Gustavo F. Doncel,[§] and T. Kyle Vanderlick*,[†]

Department of Chemical Engineering, Princeton University, Princeton, New Jersey 08544, Department of Chemical Engineering, Drexel University, Philadelphia, Pennsylvania 19104, and CONRAD Program, Department of Obstetrics and Gynecology, Eastern Virginia Medical School, 601 Colley Avenue, Norfolk, Virginia 33507

We present a steady-state and time-resolved fluorescence anisotropy analysis, using the probe diphenylhexatriene (DPH), of a hierarchical series of lipid membrane constructs that have been designed to resemble sperm plasma membranes. Anisotropy and lipid order parameters determined for the model membranes are compared to those of lipid membranes reconstituted from rabbit sperm plasma membranes. In addition, we study the response of all membrane systems to surfactant attack. The surfactants used in this investigation have current or potential use as spermicidal and antimicrobial agents. We show that our highest-level approximation of the sperm plasma membrane captures the essential characteristics of the sperm extract membranes, in terms of lipid order and response to surfactant attack. Our studies also highlight the importance of sphingomyelin as a regulator of membrane properties and also show indirect evidence of lateral phase separation in the membrane constructs that contain both cholesterol and sphingomyelin, as revealed by a preservation of lipid order under surfactant attack.

1. Introduction

Microbicidal spermicides figure prominently in contraception and the prevention of sexually transmitted diseases (STDs), especially in developing countries where the availability of condoms and other forms of protection is low and a woman's freedom of choice to use them is not always an option. Surfactant-based spermicides have found widespread use, especially those based on the nonionic surfactant nonoxynol-9 (N-9). Like all surfactants, the broad spectrum activity of N-9 is attributed to its incorporation into cellular membranes, be they eukaryotic or prokaryotic.

Of course, the tendency of surfactants to partition into membranes also puts healthy cells (e.g., vaginal and cervical epithelial) at risk. The consequences of this became glaringly clear when it was discovered that exposure to N-9 (which demonstrates Human Immunodeficiency Virus (HIV) activity in vitro) enhances the transmission of HIV.[1] Although this finding has diminished interest in surfactant-based spermicides, they remain relatively inexpensive, viable, and prominent microbicidal contraceptives. The development of more-effective surfactants for this critical health care application will rely on a firmer understanding of surfactant/membrane interactions.

Better success in identifying promising spermicidal and antimicrobial agents for clinical evaluations could be afforded by two advances: the first is the availability of an inexpensive in vitro model system, and second is the development of screening techniques to characterize the effects and mechanisms of candidate compounds. Toward this end, we have recently developed a hierarchical series of synthetic lipid mixtures designed to mimic, to various levels of sophistication, the complex lipid composition of sperm plasma membranes.[2] We have also shown how these model membranes can be used in simple vesicle leakage assays to provide one screening tool for the evaluation of surfactant candidates.[3]

While membrane leakage/permeability studies yield valuable information on the cytotoxicity of spermicidal surfactants, they do not reveal how surfactant candidates alter membrane physical properties. Fluorescence spectroscopy is a well-established technique for studying the physical properties of biological membranes,[4] because it is sensitive to the molecular motions and the local environment of the fluorescent probe. In particular, the use of time-resolved fluorescence anisotropy, for its ability to characterize both rotational dynamics as well as lipid order, has been used extensively to study membranes.[5−19]

The purpose of this work is to compare the model sperm membrane constructs to lipid membranes reconstituted from rabbit sperm plasma membranes, in terms of lipid order and the response of lipid order to surfactant attack. In doing so, we evaluate, as a screening technique for spermicidal compound candidates, the use of time-resolved fluorescence lipid order analysis, using the membrane probe diphenylhexatriene (DPH).

The rationale behind the design of these hierarchical membrane constructs has previously been discussed in detail,[2] but it is briefly described here. Because phosphatidylcholine lipids comprise the largest constituent of plasma membranes,[20] our simplest approximation of the sperm plasma membrane (construct I) is comprised of pure 1-palmitoyl-2-oleoyl-sn-glycero-3-phosphocholine (POPC). The plasma membranes of mammalian cells are rich in cholesterol (more so than most other cellular membranes).[20] Thus, our second approximation of sperm plasma membrane (construct II) is a mixture of POPC with cholesterol at a concentration of 30 mol %. The composition of construct III more closely mimics the composition of the

* To whom correspondence should be addressed. Tel.: (609) 258-4891. Fax: (609) 258-0211. E-mail: vandertk@princeton.edu.

[†] Department of Chemical Engineering, Princeton University.

[‡] Department of Chemical Engineering, Drexel University.

[§] CONRAD Program, Department of Obstetrics and Gynecology, Eastern Virginia Medical School.

10.1021/ie058084d CCC: $33.50 © 2006 American Chemical Society
Published on Web 08/29/2006

Table 1. Composition of Lipid Constructs, in Comparison to the Composition of Lipid Extracted from Rabbit Sperm Plasma Membranes (Denoted as System "X")

	Composition (mol %)							
	PC							
	16:0−22:6 di-ester	16:0−22:6 ether−ester	16:0−18:1	PE 16:0−16:0	SPH egg-SPH	PS 16:0−18:1	Chol	SGC
I			100					
II			70				30	
III	38.9		13.9	16.7	20.8	2.8		6.9
IV	28		10	12	15	2	28	5
V		28	10	12	15	2	28	5
V^-		Construct V without SGC						
X	38.3			11. 2	9.96	4.9	29.9	NA

Table 2. Surfactants Used in This Study

surfactant	type	structure
sodium dodecyl sulfate (SDS)	anionic	$CH_3(CH_2)_{11}OSO_3^-\ Na^+$
nonoxynol-9 (N-9)	non-ionic	C_9H_{19}–⟨O⟩–$(OCH_2\ CH_2)_9OH$
C31G (1:1 equimolar solution of C_{14} amine oxide and C_{16} betaine)	zwitterionic	$C_{14}H_{29}N^+(CH_3)_2O^-$ $C_{16}H_{33}N^+(CH_3)_2COO^-$
benzalkonium chloride (BZK)	cationic	⟨O⟩–$CH_2N^+(CH_3)_2R\ Cl^-$ $R = C_8H_{17}$ to $C_{18}H_{37}$

sperm cell extract membranes but without cholesterol (see Table 1). It is comprised of six commercially available lipids, including a sulfogalactosyl ceramide (SGC) that serves as an analogue for the sperm-specific glycolipid known as seminolipid.[21,22] Therefore construct III allows the isolation of the effects of cholesterol when compared to construct IV (which is the same complex mixture of lipids in construct III with the addition of cholesterol). Constructs IV and V are high-level models of the composition of the sperm plasma membrane and were designed to determine the effects of ether−ester linked phospholipids that are intrinsic to sperm plasma membranes;[23] construct V contains these unusual lipids, while construct IV contains instead analogous ester−ester linked lipids. We note that these lipids bear a high degree of chain unsaturation. Construct V^- is compositionally similar to construct V, but with the negatively charged sulfogalactolipid removed to isolate the effects of this analogue sperm-specific membrane component on membrane properties. The lipid membrane isolated from the anterior head of rabbit spermatozoa, which we reference herein as construct X, is used as a basis to compare the model lipid constructs. (For a detailed compositional description of the rabbit sperm plasma membrane extract, see our previous study.[2]) A simple breakdown of the core components of all membranes used in these studies is listed in Table 1.

As a basis for this current investigation, we study the interactions of the model membranes with four surfactant candidates, shown in Table 2: (1) nonoxynol-9 (N-9), which is a nonionic surfactant already widely used as a spermicidal agent;[24] (2) C31G, which is an amphoteric mixture of two surface-active molecules, C_{14} alkylamine oxide and C_{16} alkyl betaine;[25] (3) benzalkonium chloride (BZK), which is a vaginal spermicide[26] used worldwide; and (4) sodium dodecyl sulfate (SDS), which is an anionic surfactant with protein denaturing antiviral activities.[27]

2. Materials and Methods

2.1. Materials. 1-Palmitoyl-2-oleoyl-*sn*-glycero-3-phosphocholine (POPC), brain sulfatide (SCG), 1-palmitoyl-2-docosahexaenoyl-*sn*-glycero-3-phosphocholine (16:0−22:6 ester−ester PC), 1-alkyl-2-acyl-*sn*-glycero-3-phosphocholine (16:0−22:6 ether−ester PC), 1,2-dipalmitoyl-*sn*-glycero-3-phosphoethanolamine (DPPE), 1-palmitoyl-2-oleoyl-*sn*-glycero-3-[phospho-L-serine] (POPS), egg-sphingomyelin (SPH), and cholesterol (Chol) were purchased from Avanti Polar Lipids (Birmingham, AL). Benzalkonium chloride (BZK), sodium dodecyl sulfate, (SDS), *N*-2-hydroxyethylpiperazine−*N*′-2-ethanesulfonic acid (HEPES), sodium chloride (NaCl), 2-(4-biphenyl)-5-(4-*tert*-butyl-phenyl)-1,3,4-oxadiazole, and tetrahydrofuran (THF) were obtained from Sigma (St. Louis, MO). C31G (equimolar mixture of C_{14} amine oxide and C_{16} alkyl betaine at purities of 88.7% and 98.2%, respectively) was obtained from Biosyn (Philadelphia, PA). Nonoxynol-9 (N-9) was obtained from Biosyn (as Rhone-Poulenc's Igepal CO-630 Special at a purity of 95%). DPH was purchased from Molecular Probes (Eugene, OR). All chemical were used without further purification.

2.2. Preparation of Surfactant and Buffer Solutions. The buffer used in this study is 16.66 mM HEPES and 125 mM NaCl, pH adjusted to 7.4, and the osmolarity has been adjusted to 265 mOs (Fiske Micro-Osmometer Model 210). All aqueous solutions were prepared using Millipore water. Stock solutions (30 mM) of the spermicidal surfactants SDS, BZK, N-9, and C31G in buffer were prepared, vortex-mixed (5 min), and bath-sonicated (5 min).

2.3. Isolation of Rabbit Sperm Plasma Membranes. To isolate the plasma membrane from the anterior head of rabbit spermatozoa, we used a modified version of the method reported by Wolf et al.[28] The details of the membrane extraction procedure have been described previously, but we will be briefly review them here. Washed sperm samples from adult male White New Zealand rabbits were combined and centrifuged at 1200 g for 20 min in Dulbecco's phosphate buffer solution. The saline was removed, and this washing procedure was repeated three times in total. The pellet was cooled to 4 °C and remained at this temperature over the duration of the process. The pellet was resuspended 10 times in Ca^{2+}- and Mg^{2+}-free Hank's balanced solution. The sperm solution was then treated to nitrogen cavitation in a Parr Instrument cell disruption bomb that was packed in ice. The bomb pressure was 750 psi for 10 min. The suspension was then centrifuged for 10 min at 6000 g, and the supernatant was additionally centrifuged for 30 min at 100 000 g. The remaining pellet was resuspended in Hanks

solution and centrifuged at 10 000 g for 10 min. Lipids were extracted with a 2:1 methanol−chloroform solution, and the bottom phase was collected and dried in a rotary evaporator.

2.4. Vesicle Preparation and Characterization. Large unilamellar vesicles were prepared by film deposition and high-pressure extrusion. Briefly, stock solutions of lipids in chloroform and DPH in THF were mixed to achieve the desired compositions (listed in Table 1). DPH was incorporated into the lipid mixtures at a lipid/DPH ratio of 200, which was selected to be high enough to give sufficient fluorescence intensity but low enough to avoid loss of anisotropy due to homo-transfer. The mixing was conducted in 20-mL scintillation vials, and solvent was removed under a stream of nitrogen in a rotary evaporator. The samples were then placed in a vacuum oven at room temperature and a pressure of 28 in. of Hg for 24 h. After the solvent removal, the lipid films were hydrated with the appropriate amount of buffer to give a total lipid concentration of 2.5mM. Samples were then vortex-mixed for 5 min and subjected to five freeze−thaw cycles (using liquid nitrogen). The multilamellar membrane dispersions were then extruded (Northern Lipids, Inc.) through 400-nm (5 passes) and 100-nm (10 passes) polycarbonate filters (Nucleopore). Aliquots of these large unilamellar vesicles were diluted in buffer to a final concentration of 0.5 mM. The effective diameter of the large unilamellar vesicles was determined to be 109 ± 14 nm by dynamic light scattering (Brookhaven 90plus DLS, 15mW laser at 678 nm, BI-9000-AT digital autocorrelator). The size distribution was determined to be reasonably monodisperse, with a mean polydispersity of 0.09 ± 0.034. All scattering measurements were conducted at 25 °C and at a scattering angle of 90°.

2.5. Steady-State Fluorescence Measurements. All steady-state fluorescence measurements were made on a Photon Technology International, Inc., Model A-710 system with the band pass set to 2 nm. The temperature of the sample chamber was controlled to ±0.5 °C via a circulating water bath, and the temperature was monitored with a cuvette thermometer (Fisher Corp., Philadelphia, PA, Model 15-078J). DPH in the sperm cell membrane model constructs was excited at 363 nm, and the emission was measured at 426 nm. The steady-state DPH anisotropy was determined by measuring the vertically and horizontally polarized components of the fluorescence emission with both vertically and horizontally polarized excitation using motorized Glan−Thompson polarizers, as a function of time. Fluorescence intensities were recorded at an integration rate of 0.25 point/s for durations of 120 s. The steady-state anisotropy (R_{ss}) is calculated using eq 1, with the intensities averaged over the 120 s acquisition:

$$R_{ss} = \frac{I_{vv} - GI_{vh}}{I_{vv} + 2GI_{vh}} \tag{1}$$

$$G = \frac{I_{hv}}{I_{hh}} \tag{2}$$

Here, I_{vv} is the intensity with vertical excitation and vertical emission, I_{vh} is the intensity with vertical excitation and horizontal emission, and G is defined as the ratio of the intensity with horizontal excitation and vertical emission to the intensity with horizontal excitation and horizontal emission.

The orientation of the polarizers was calibrated by measuring the anisotropy of a dilute scattering solution (100 nm Duke Standard in deionized (DI) water) and was determined to be 0.96.

2.6. Time-Resolved Fluorescence Measurements. All time-resolved fluorescence measurements were conducted on a Photon Technology International, Model C-71 system (time domain, stroboscopic detection system). The excitation source was a pulsed nitrogen laser that was operating (Photon Technology International, Model GL-3300) at 337 nm at a frequency of 10 Hz. This excitation source was used to excite a dye laser (Photon Technology International, Model GL-302), and the dye used in this study was 0.004 M 2-(4-biphenyl)-5-(4-*tert*-butylphenyl)-1,3,4-oxadiazole in toluene. The samples were excited at 363 nm, and the DPH emission was measured at 426 nm; monochromatic excitation and emission were obtained using diffraction-grating monochromators. The polarized emission was recorded in intervals of 500 ps over a range of 100 ns in random acquisition mode, with the reported intensity at each time interval being the average of 25 separate laser pulses. The instrument response function was recorded by measuring the intensity decay at 363 nm of a dilute scatting solution (100 nm Duke Standard in DI water). The intensity of the instrument response function was controlled with neutral density filters.

2.7. Analysis of DPH Anisotropy Decay Kinetics. For each membrane construct listed in Table 1, we measured the system response under four separate polarizer conditions: vertically polarized excitation and vertically polarized emission (M_{vv}), vertically polarized excitation and horizontally polarized emission (M_{vh}), horizontally polarized excitation and vertically polarized emission (M_{hv}), and horizontally polarized excitation and horizontally polarized emission (M_{hh}). The actual DPH fluorescence decay ($I(t)$) is assumed to follow a double exponential model, as shown below, and the parameters are determined by iteratively reconvoluting this function with the measured lamp response to fit the system response (as done by the TimeMaster analysis software package).

$$I(t) = \alpha_1 e^{-t/\tau_1} + \alpha_2 e^{-t/\tau_2} \tag{3}$$

To reduce the number of fitted parameters, the TimeMaster analysis package uses a global analysis method, which constrains the decay times τ_1 and τ_2 to be the same in the I_{vv} and I_{vh} decay models. The factor G is calculated by averaging the ratio of M_{hv} to M_{hh}, as shown in eq 4:

$$G = \left\langle \frac{M_{hv}(t)}{M_{hh}(t)} \right\rangle \tag{4}$$

$$r(t) = \frac{I_{vv}(t) - GI_{vh}(t)}{I_{vv}(t) + 2GI_{vh}(t)} \tag{5}$$

This factor is used to correct for the fact that monochromators do not equally transmit polarized components of light. The decay of anisotropy ($r(t)$) is calculated using the best-fit double exponential decay models and G with eq 5.

To extract the anisotropy decay parameters, the numerical results of eq 5 are fit by minimizing the sum of the squared errors with the hindered rotor model, which assumes a single rotational correlation time and a nonzero limiting anisotropy:

$$r(t) = (r_0 - r_\infty)e^{-(t/\varphi)} + r_\infty \tag{6}$$

Here, $r(t)$ is the DPH anisotropy as a function of time during the fluorescence decay, r_0 the anisotropy at time zero, r_∞ the anisotropy at infinite time or the limiting anisotropy, and φ the rotational correlation time.

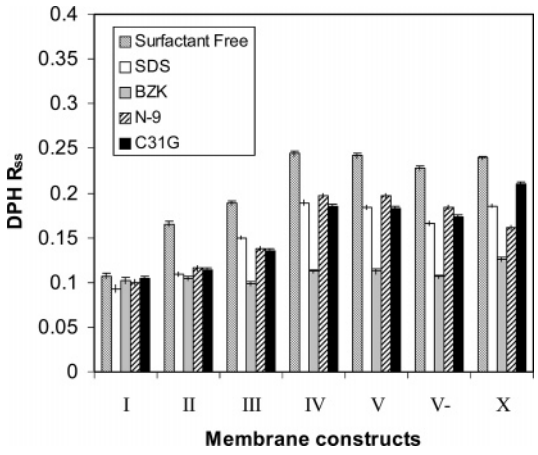

Figure 1. Steady-state diphenylhexatriene (DPH) anisotropy in sperm cell membrane model constructs at 28 °C show that the high-level constructs IV and V are reasonable models of the sperm plasma membrane and display similar response to surfactant attack. In all cases, the surfactant-to-lipid ratio is 2. Under these conditions, BZK is the most effective in regard to reducing the DPH anisotropy.

The lipid order parameter is related to the "best-fit" anisotropy decay parameters, as shown below.[16]

$$S = \left(\frac{r_\infty}{r_0}\right)^{1/2} \tag{7}$$

The lipid order parameter is independent of the model used to determine the rotational correlation times of the decays of anisotropy, because the limiting anisotropy is independent of the number of assumed rotational correlation times; furthermore, the values of the limiting anisotropies are readily determined from the experimental anisotropy decay data. In practice, it is useful to define the effective lipid order parameter (S_{eff}), where r_0 is set equal to 0.4.

3. Results

3.1. Steady-State DPH Anisotropy Studies. To characterize the effect of membrane composition on the resistance to rotational motions of the fluidity probe DPH, we measured the steady-state fluorescence anisotropy of DPH, R_{ss}, at 28 °C in the model membrane constructs and the rabbit sperm extract membranes. With no surfactant present, the steady-state DPH anisotropies are 0.107, 0.165, 0.189, 0.244, 0.242, 0.228, and 0.239 for membrane constructs I, II, III, IV, V, V^-, and X of the sperm cell extract membranes, respectively.

The effects of surfactant attack by SDS, BZK, N-9, and C31G on the fluidity of these membranes was determined by measuring the steady-state DPH anisotropy after 24-h incubation with the surfactants at a lipid-to-surfactant ratio of 1:2. Results are shown in Figure 1. As is readily seen, except for the extremely simple POPC membranes (construct I), surfactant incorporation causes a significant decrease in steady-state anisotropy. Although easy to perform, steady-state fluorescence anisotropy provides time-averaged information on the resistance to rotational motions but cannot decouple the dynamic contribution to anisotropy (that originates from the viscous drag of the fluorescent probe with the surrounding lipid molecules) from the static contribution (that reflects the order of the local lipid environment around the probe).

3.2. Time-Resolved DPH Anisotropy Kinetics. To further characterize the membrane properties of the model sperm plasma membranes and the effects of the spermicidal surfactants, we measured the time-resolved decay of DPH anisotropy at 28 °C in the model constructs and the extract membranes with and without the spermicidal surfactant candidates SDS, BZK, N-9, and C31G.

Table 3. DPH Anisotropy Decay Parameters before and after 24 h Incubation with Spermicidal Surfactant in Model Sperm Plasma Membrane Constructs and Extract Membranes (Surfactant-to-Lipid Ratio = 2, T = 28 °C)

	r_0	ϕ (ns)	r_∞
II	0.201 ± 0.014	4.45 ± 0.74	0.1295 ± 0.0006
II^{SDS}	0.191 ± 0.019	5.79 ± 0.95	0.0393 ± 0.0046
II^{BZK}	0.329 ± 0.032	2.88 ± 0.22	0.0044 ± 0.0044
II^{N-9}	0.306 ± 0.027	4.21 ± 0.51	0.0097 ± 0.0042
II^{C31G}	0.222 ± 0.026	4.17 ± 0.84	0.0361 ± 0.0025
III	0.201 ± 0.041	3.41 ± 2.80	0.1384 ± 0.0026
III^{SDS}	0.201 ± 0.016	4.30 ± 1.03	0.1220 ± 0.0017
III^{BZK}	0.231 ± 0.043	4.74 ± 0.87	0.0035 ± 0.0035
III^{N-9}	0.286 ± 0.054	3.50 ± 1.05	0.0818 ± 0.0015
III^{C31G}	0.251 ± 0.026	5.08 ± 0.94	0.0745 ± 0.0027
V	0.266 ± 0.011	4.14 ± 1.06	0.2158 ± 0.0015
V^{SDS}	0.268 ± 0.047	3.23 ± 1.63	0.1635 ± 0.0057
V^{BZK}	0.251 ± 0.047	4.65 ± 1.20	0.0367 ± 0.0047
V^{N-9}	0.349 ± 0.080	2.37 ± 1.03	0.1627 ± 0.0044
V^{C31G}	0.249 ± 0.014	5.00 ± 0.63	0.1337 ± 0.0015
X	0.243 ± 0.007	5.49 ± 0.85	0.2185 ± 0.0031
X^{SDS}	0.220 ± 0.018	3.10 ± 0.61	0.1564 ± 0.0026
X^{BZK}	0.178 ± 0.015	6.01 ± 0.83	0.0564 ± 0.0023
X^{N-9}	0.212 ± 0.020	4.50 ± 0.51	0.1076 ± 0.0023
X^{C31G}	0.254 ± 0.014	3.38 ± 0.63	0.1935 ± 0.0010

To analyze anisotropy decay, we used the hindered rotor model.[4] In this model, the anisotropy at time zero r_0 (also know as the fundamental anisotropy), the rotational correlation time φ, and the limiting anisotropy r_∞ can be determined by fitting the experimentally determined anisotropy decays (eq 6), using the method of nonlinear least squares. The hindered rotor model was determined to describe the experimentally determined decays of anisotropies in this study adequately; thus, the use of multiple rotational correlation time models were not justified.

The determined decays of anisotropy were determined to be sensitive to the data range over which the global I_{vv} and I_{vh} fits were conducted. Consequently, we performed a sensitivity analysis that varied the fitting range: 37−90 ns, 37−100 ns, 37−110 ns, 37−115 ns, and 37−120 ns. Larger ranges of data that were used for the fits resulted in longer extracted rotational correlation times. The results reported for the decay of anisotropy model (eq 6) are the average values of these five fitting ranges. In all cases, the fits were deemed acceptable if the global χ^2 and the individual χ^2 values for the I_{vv} and I_{vh} fits were all $<$1.2. The best-fit model parameters for the I_{vv} and I_{vh} decays were determined to be insensitive to the initial guess values for the fluorescence decay times (τ_1 and τ_2): the initial values used in this study were 2 ns and 11 ns.

Anisotropy decays with and without surfactant incubation are listed in Table 3 (given only for a subset of the many systems examined). The fundamental anisotropies, r_0, range from 0.18 to 0.35 for the model constructs and the extract membranes with and without surfactant incubation. Theoretically, the fundamental anisotropy for probes whose absorption and emission transition moments are parallel (such as those for DPH) is 0.4.[4,16] However, experimentally values of r_0 lower than 0.4 are often obtained.[5] This difference has been attributed to sub-nanosecond rate processes that are beyond resolution and a loss of anisotropy that is due to scattered light effects.[29] As seen in Table 3, the values for the rotational correlation times are approximately constant at 4 ns for all of the membrane constructs, both with and without surfactant incubation, and are consistent with other reported literature values.[5] This indicates that changes observed in the steady-state anisotropy data, as a function of membrane

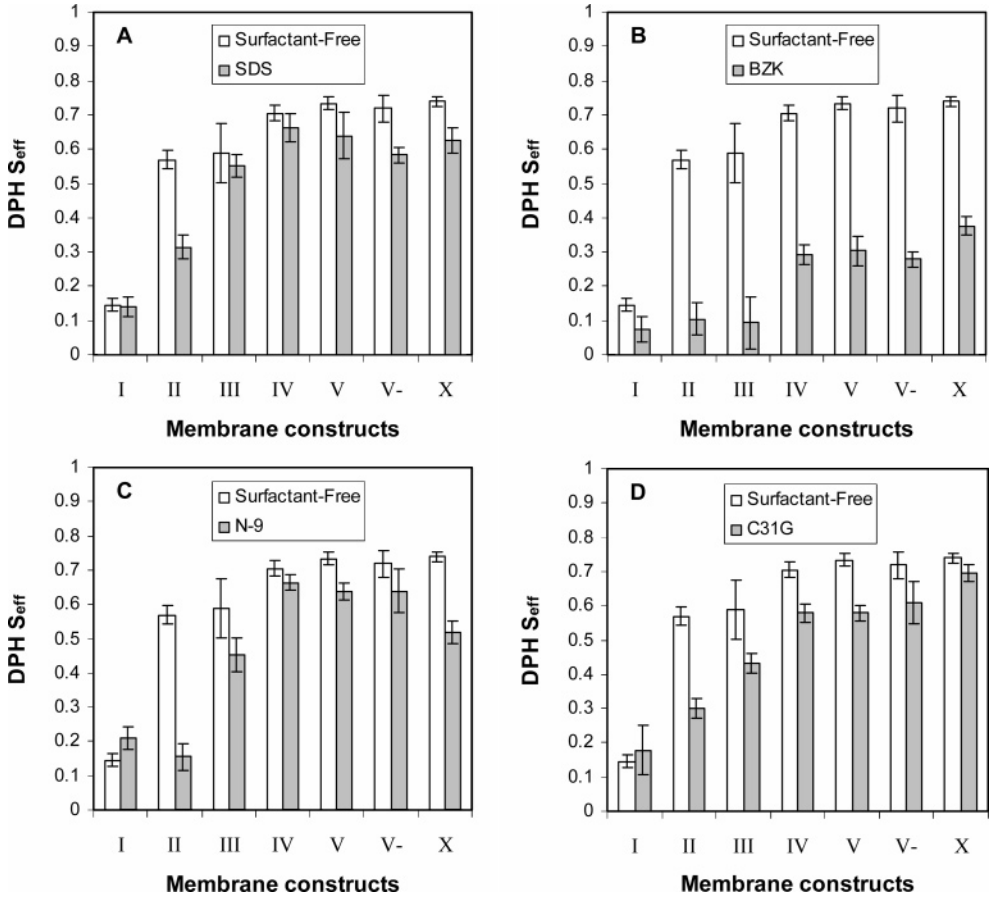

Figure 2. Effective DPH lipid order parameter (S_{eff}) in the hierarchy of lipid constructs for the sperm plasma membrane and the rabbit sperm cell extract membranes without (white bars) and with (shaded bars) 24 h of incubation with the spermicidal surfactants: (a) SDS (anionic), (b) BZK (cationic), (c) N-9 (non ionic), and (d) C31G (zwitterionic) at 28 °C. The surfactant-to-lipid ratio is 2.

composition and surfactant incorporation, are not primarily rate-controlled. Rather, these changes are predominately due to the static contribution to anisotropy (lipid acyl chain order).

3.3. DPH Lipid Order Parameter Studies. The effective DPH lipid order parameters were calculated from the r_∞ values using eq 7 (with $r_0 = 0.4$) and are plotted in Figure 2a, b, c, and d for SDS, BZK, N-9, and C31G, respectively. The lipid order parameters determined in membranes free of surfactant are also shown in Figure 2. These S_{eff} values range from 0.146 for the simple POPC membrane (construct I) to a maximum value of 0.739 for the rabbit sperm lipid extract membranes (construct X).

In all membranes, the incorporation of surfactant (of any type) resulted in a decrease in lipid order parameter. SDS reduced the S_{eff} value of construct II by 45%; SDS had a negligible effect (~5% reduction) on constructs I, III, and IV, and it caused similar reductions for the extract (15%) and the highest-level construct V (13%). It is evident, from Figure 2b, that, at a surfactant-to-lipid ratio of 2, BZK is the most effective, in regard to reducing the DPH lipid order parameter, specifically for constructs II and III, where the reduction is >80%. It is interesting to note that the higher-order constructs IV thru V$^-$ (which contain both cholesterol and sphingomyelin) and the extract membranes maintain a S_{eff} value of at least 0.28 under this level of surfactant attack. Incubation with N-9 resulted in a 43% increase in S_{eff} for construct I, while causing a 73% decrease in S_{eff} for construct II, and a 23% decrease in the cholesterol-free, sphingomyelin-rich construct III. The higher-order model constructs VI thru V$^-$ responded similarly to the N-9 attack, with an approximate average decrease in S_{eff} of ~10%, which is significantly less than the reduction observed in the extracts (30%). In contrast, the incorporation of C31G had a more pronounced effect on the higher-level constructs (18% reduction) than on the natural lipid extract membranes (6% reduction).

4. Discussion

In this work, we performed a steady-state and time-resolved fluorescence anisotropy study of the membrane probe DPH in a series of model lipid constructs (that mimic the sperm plasma membrane) and in reconstituted rabbit sperm plasma lipid membranes. This series of membrane constructs was designed to test the effects of composition on the physical properties of sperm plasma membranes and their interactions with spermicidal surfactants. We compared these sperm plasma membrane models in terms of lipid order using time-resolved fluorescence anisotropy. The surfactant candidates used in this investigation were selected because they have current or potential use as spermicidal agents and are representative of four separate surfactant classes: anionic (SDS), cationic (BZK), nonionic (N-9), and zwitterionic (C31G).

4.1. Characterization of the Hierarchy of Membrane Constructs. The effect of cholesterol on the DPH lipid order parameter is clearly evident by the increase in S_{eff} for construct II (POPG and Chol) compared to construct I (POPG). (See Figure 2.) This increase in lipid order is a direct result of the presence of the rigid cholesterol molecules within the membrane, causing the phospholipid acyl chains to adopt all-trans rotomer configurations[12,30] and the bilayer thickness to increase by as much as 10%−15%.[31] This same trend is also observed (although to a lesser extent) in the more-complex lipid constructs

III (cholesterol-free) and IV (construct III with cholesterol) by an increase in S_{eff} (see Figure 2).

Interestingly, the cholesterol-free construct III exhibited an S_{eff} value (0.588) that was comparable to that of construct II (0.569), which contains 30 mol % cholesterol. This demonstrates the profound effect that sphingomyelin has, even in the absence of cholesterol, on the regulation of membrane properties and demonstrates that sphingomyelin, even in minority amounts, induces chain order and probably also increases the bilayer thickness.

In this study, no significant difference in either R_{ss} (Figure 1) or S_{eff} (Figure 2) was observed between construct V, which contains the ether−ester linkage phosphatidylcholine intrinsic to sperm plasma membranes, and construct IV, which contains, instead, the analogous lipid with a convention ester−ester linkage. This is most likely due to the DPH probe locating itself deep in the hydrophobic core of the bilayer and therefore not experiencing the differences (if any) between these two lipid types. We suspect the membrane probe TMA−DPH, which partitions at the hydrophilic/hydrophobic interface, would be more sensitive to differences between the ether−ester linkage and the ester−ester linkage.

Construct V^- is identical in composition to construct V, except with the sulfogalactolipid removed, and it was designed to determine the effect of these negatively charged species (analogue to seminolipid) on membrane properties. Figure 2 clearly shows that the removal of this component has no major effect on DPH lipid order. This, again, may be due to the location of the DPH probe, relative to the unique headgroup of this lipid species.

Most importantly, the high-level constructs (IV thru V^-) match the DPH lipid order of the sperm extract membranes quite well (with values of the S_{eff} approximately equal to that of the sperm extract membranes, ~0.72). Steady-state anisotropy measurements also match up well. Of all the membrane components varied in this study, we conclude that the combination of sphingomyelin and cholesterol bears large responsibility for the quantitative agreement in DPH lipid order parameter results between the high-level constructs (IV, V, and V^-) and the extract sperm plasma membranes (X).

4.2. Response to Surfactant Attack. To further characterize and compare the hierarchy of lipid constructs to the rabbit sperm plasma membrane extract, we measured the DPH lipid order parameter in the membrane samples after 24 h of incubation with four different spermicidal surfactants (SDS, BZK, N-9, and C31G). As a basis of comparison for the surfactant studies, the surfactant-to-lipid ratio was fixed at a value of 2. This ratio yielded a good signal-to-noise ratio, and it was more than sufficient to generate differences between the systems that have been studied. Because the main focus of this work was on the membrane systems and their general response to surfactant attack, it is difficult to learn much about the details of specific surfactant−membrane interactions under the very limited conditions explored. Nevertheless, several interesting results emerged.

Most obviously, all surfactants, regardless of type, serve to decrease significantly membrane lipid order within the deep hydrophobic core of the membrane (where the DPH locates). Longer-chained surfactants would be more naturally prone to creating disorder therein, and this is likely one factor responsible for the relative responses of the longer-chained surfactant systems (C31G and BZK), compared to the others (SDS and N-9).

Of the four surfactants investigated, the cationic BZK is the most membrane perturbing, as quantified by the reduction in the lipid order parameter (see Figure 2b). Charge effects probably account for some of this activity. Although net neutral, even POPG membranes exhibit a negative surface potential.[32] However, favorable electrostatics is not the only factor that underpins the effectiveness of BZK, because the removal of anionic lipids (present in V but not in V^-) diminishes the activity of the surfactant only slightly. Further studies are needed to uncover the molecular features and interactions responsible for the distinctive behavior of this particular surfactant.

Of the remaining surfactants, the order of effectiveness in perturbing the lipid extracts membranes was N-9 > SDS > C31G. Although the level of disorder is similar to that observed in the higher-level constructs, it is clear that interactions with specific components of the natural membrane system that are not present in the model constructs are important. These interactions lead to significant differences in behavior between these three surfactants and between the extract system and model constructs. N-9 causes more disorder in the natural system than in the high-level constructs; the opposite is true for C31G.

Regardless of surfactant type, we find that the combination of sphingomyelin and cholesterol in our high-level constructs provide a preservation of lipid order from surfactant attack that neither sphingomyelin nor cholesterol alone can provide. We believe that this preservation of lipid order is indirect evidence of cholesterol/sphingomyelin-rich domains[33,34] in the high-level constructs VI, V, V^-, and in the sperm extract membranes. The high concentration of 16:0−22:6 PC found in sperm cell plasma membranes may well serve to promote the formation of laterally phase separated domains. We imagine that the 16:0−22:6 PC acts as a "line-actant", where the fully saturated (16:0) chain partitions at the sphingomyelin/cholesterol domain interface and the unsaturated (22:6) chain partitions facing the continuous fluid lipid phase, thus stabilizing the domain within the membrane. Further investigations are needed to confirm the presence of "detergent-resistant" raft-like domains enriched in cholesterol and sphingomyelin. The roles of these domains on cell function is not presently well understood, but they have been implicated in cellular signaling. Hence, studies of these domains in sperm membranes may lead to novel routes of contraception.

5. Summary and Conclusions

We conducted a time-resolved diphenylhexatriene (DPH) lipid order study of a series of lipid constructs that mimic the sperm plasma membrane. These model sperm systems were designed to study the role of lipid composition on membrane properties and interactions with spermicidal/antimicrobial agents. We observed that the static contribution dominates the steady-state anisotropy values (see Table 3 and Figure 2) and that sphingomyelin, combined with cholesterol, determines the lipid order in these sperm plasma membrane model systems. The highest-level constructs (IV thru V^-) demonstrated the most resistance to the surfactant-induced reduction of lipid order (see Figure 2). Our results provided indirect evidence of cholesterol/sphingomyelin-rich domains in both the extract membranes and the high-level constructs.

This work also validates that the highest-level model membrane (construct V) is a good approximation of the sperm plasma membrane, in terms of lipid order and response to surfactant attack.

The use of DPH anisotropy is well-suited for the investigation of interactions of spermicidal/antimicrobial candidate compounds, because lipid order is a very sensitive to membrane composition and surfactant-induced membrane perturbation. The trends observed in time-resolved measurements are directly

reflected in the steady-state anisotropy measurements, which suggests that the latter would serve well as a simple and relatively inexpensive tool for screening candidate compounds.

Acknowledgment

Support for this subproject [GMP-01-25] was provided by the Global Microbicide Project (GMP) of the CONRAD Program, Eastern Virginia Medical School. The views expressed by the authors do not necessarily reflect the views of the CONRAD Program or GMP. The authors are especially delighted to submit this paper in honor of Bill Russel, whose presence at Princeton provides us with constant inspiration for scholarship of the highest caliber.

Literature Cited

(1) Van Damme, L.; Ramjee, G.; Alary, M.; Vuylsteke, B.; Chandeying, V.; Rees, H.; Sirivongrangson, P.; Mukenge-Tshibaka, L.; Ettiegne-Traore, V.; Uaheowitchai, C.; Karim, S. S.; Masse, B.; Perriens, J.; Laga, M. Effectiveness of COL-1492, a nonoxynol-9 vaginal gel, on HIV-1 transmission in female sex workers: A randomised controlled trial. *Lancet* **2002**, *360*, 971−977.

(2) Apel-Paz, M.; Vanderlick, T. K.; Chandra, N.; Doncel, G. F. A hierarchy of lipid constructs for the sperm plasma membrane. *Biochem. Biophys. Res. Commun.* **2003**, *309*, 724.

(3) Apel-Paz, M.; Doncel, G. F.; Vanderlick, T. K. Membrane perturbation by surfactants candidates for STD prevention. *Langmuir* **2003**, *19*, 591.

(4) Lakowicz, J. R. *Principles of Fluorescence Spectroscopy*; Kluwer Academic/Plenum Publishers: New York, 1999.

(5) Veatch, W. R.; Stryer, L. Effect of cholesterol on the rotational mobility of diphenylhexatriene in liposomes: a nanosecond fluorescence anisotropy study. *J. Mol. Biol.* **1977**, *117*, 1109.

(6) Straume, M.; Litman, B. J. Influence of cholesterol on equilibrium and dynamic bilayer structure of unsaturated acyl chain phosphatidylcholine vesicles as determined from higher order analysis of fluorescence anisotropy decay. *Biochemistry* **1987**, *26*, 5121.

(7) Vijayasarathay, S.; Shivaji, S.; Balaram, P. Bull sperm plasma and acrosomal membranes: fluorescence studies of lipid phase fluidity. *Biochem. Biophys. Res. Commun.* **1982**, *108*, 585.

(8) Velez, M.; Pilar-Lillo, M.; Ulises-Acuna, A.; Gonzalez-Rodriguez, J. Cholesterol effect on the physical state of lipid multibilayers from the platelet plasma membrane by time-resolved fluorescence. *Biochim. Biophys. Acta* **1995**, *1235*, 343.

(9) Haidl, G.; Opper, C. Changes in lipids and membrane anisotropy in human spermatozoa during epididymal maturation. *Hum. Reprod.* **1997**, *12*, 2720.

(10) Stubbs, C. D.; Kouyama, T.; Kinosita, K., Jr.; Ikegami, A. Effect of double bonds on the dynamic properties of the hydrocarbon region of lecithin bilayers. *Biochemistry* **1981**, *20*, 4257.

(11) Dale, R. E.; Chen, L. A.; Brand, L. Rotational relaxation of the "microviscosity" probe diphenylhexatriene in paraffin oil and egg lecithin. *J. Biol. Chem.* **1977**, *252*, 7500.

(12) Kawato, S.; Kinosita, K., Jr.; Ikegami, A. Effect of cholesterol on the molecular motion in the hydrocarbon region of lecithin bilayers studied by nanosecond fluorescence techniques. *Biochemistry* **1987**, *17*, 5026.

(13) Kawato, S.; Kinosita, K.; Ikegami, A. Dynamic structure of lipid bilayers studied by nanosecond fluorescence techniques. *Biochemistry* **1977**, *16*, 2319.

(14) Kinosita, K., Jr.; Kataoka, R.; Kimura, Y.; Gotoh, O.; Ikegami, A. Dynamic structure of biological membranes as probed by 1,6-diphenyl-1,3,5-hexatriene: a nanosecond fluorescence depolarization study. *Biochemistry* **1981**, *20*, 4270.

(15) Engel, L. W.; Pendergast, F. G. Values for and significance of order parameters and cone angles of fluorophore rotation in lipid bilayers. *Biochemistry* **1981**, *20*, 7338.

(16) Heyn, M. P. Determination of lipid order parameters and rotational correlation times from fluorescence depolarization experiments. *FEBS Lett.* **1979**, *108*, 359.

(17) Hinkovska-Galcheva, V.; Srivastava, P. N. Phospholipids of rabbit and bull sperm membranes: structural order parameter and steady-state fluorescence anisotropy of membranes and membrane leaflets. *Mol. Reprod. Dev.* **1993**, *35*, 209.

(18) Ladha, S. Lipid heterogeneity and membrane fluidity in a highly polarized cell, the mammalian spermatozoon. *J. Membr. Biol.* **1998**, *165*, 1.

(19) Shinitzky, M.; Barenholz, Y. Fluidity parameters of lipid regions determined by fluorescence polarization. *Biochim. Biophys. Acta* **1978**, *515*, 367.

(20) Genis, R. B. *Biomembranes Molecular Structure and Function*; Springer−Verlag: New York, 1989.

(21) Attar, M.; Katers, M.; Khalil, M. B.; Carreier, D.; Wong, P. T. T.; Tanphaichitr, N. A Fourier transform infrared study of the interaction between germ-cell specific sulfogalactosylglycerolipid and dimyristoylglycerophosphocholine. *Chem. Phys. Lipids* **2000**, *106*, 101.

(22) Tupper, S.; Wong, P. T. T.; Kates, M.; Tanphaichitr, N. Interaction of divalent-cations with germ-cell specific sulfogalactosylglycerolipid and the effects on lipid chain dynamics. *Biochemistry* **1994**, *33*, 13250.

(23) Flesch, F. M.; Gadella, B. M. Dynamics of the mammalian sperm plasma membrane in the process of fertilization. *Biochim. Biophys. Acta* **2000**, *1469*, 197.

(24) Hillier, S. L.; Moench, T.; Shattock, R.; Black, R.; Reichelderfer, P.; Veronese, F. In Vitro and In Vivo: The Story of Nonoxynol 9. *J. Acquired Immune Defic. Syndr.* **2005**, *39*, 1.

(25) Corner, A. M.; Dolan, M. M.; Yankell, S. L.; Malamud, D. C31g, a New Agent for Oral Use with Potent Antimicrobial and Antiadherence Properties. *Antimicrob. Agents Chemother.* **1988**, *32*, 350.

(26) Mendez, F.; Castro, A.; Ortega, A. Use Effectivness of a Spermicidal Suppository Containing Benzalkonium Chloride. *Contraception* **1986**, *34*, 353.

(27) Howett, M. K.; Neely, E. B.; Christensen, N. D.; Wigdahl, B.; Krebs, F. C.; Malamud, D.; Patrick, S. D.; Pickel, M. D.; Welsh, P. A.; Reed, C. A.; Ward, M. G.; Budgeon, L. R.; Kreider, J. W. A Broad-Spectrum Microbicide with Virucidal Activity against Sexually Transmitted Viruses. *Antimicrob. Agents Chemother.* **1999**, *43*, 314.

(28) Wolf, D. E.; Lipscomb, A. C.; Maynard, V. M. Causes of non diffusing lipid in the plasma-membrane of mammalian spermatozoa. *Biochemistry* **1988**, *27*, 860.

(29) Lentz, B. R.; Moore, B. M.; Barrow, D. A. Light-scattering effects in the measurement of membrane microviscosity with diphenylhexatriene. *Biophys. J.* **1979**, *25*, 489.

(30) Feingold, L. *Cholesterol in Membrane Models*; CRC Press: Boca Raton, FL, 1993.

(31) Nezil, F. A.; Bloom, M. Combined influence of cholesterol and synthetic amphiphillic peptides upon bilayer thickness in model membranes. *Biophys. J.* **1992**, *61*, 1176.

(32) Cummings, J. E.; Satchell, D. P.; Shirafuji, Y.; Ouellette, A. J.; Vanderlick, T. K. Electrostatically Controlled Interactions of Mouse Paneth Cell Alpha-Defensins with Phospholipid Membranes. *Australian J. Chem.* **2003**, *56*, 1031.

(33) Brown, D. A.; London, E. Functions of lipid rafts in biological membranes. *Annu. Rev. Cell Dev. Biol.* **1998**, *14*, 111.

(34) Wolf, D. E.; Maynard, V. M.; McKinnon, C. A.; Melchior, D. L. Lipid domains in the ram sperm plasma membrane demonstrated by differential scanning calorimetry. *Proc. Natl. Acad. Sci. U.S.A.* **1990**, *87*, 6893−6896.

Received for review November 29, 2005
Accepted July 27, 2006

IE058084D